Journal of Ceramic Processing Research. Vol. 11, No. 5, pp. 631~635 (2010)

J O U R N A L O F
Ceramic Processing Research

Synthesis and characterization of TiO_2-ZnO nanocomposite by a two-step chemical method

Chang Sung Lim*
Dept. of Advanced Materials Science and Engineering, Hanseo University, Seosan 356-706, Korea

Nanocrystlline TiO_2 coated ZnO particles were synthesized by a two-step chemical method, which were prepared by the polymerization of ZnO nanoparticles and followed by a sol-gel coating with a TiO_2 nanolayer. The variation in zeta potential of ZnO and TiO_2 with pH exhibited isoelectric points (IEP) at 9.3 and 3.5, respectively. The ZnO particles coated with TiO_2 nanoparticles show a uniformly dispersed morphology without any agglomeration. The average particle size of ZnO particles coated with TiO_2 particles was approximately 120-140 nm. The size of the ZnO particles was 100 nm and the size of the TiO_2 coating was below 10-20 nm. The size, morphology, composition and structure of the nanocrystalline TiO_2 coated ZnO particles were characterized by TG/DTA, XRD, SEM, EDS and TEM in detail.

Key words: Nanocrystalline, TiO_2 coated ZnO, two-step chemical method, interdependent attraction.

Introduction

In recent years, semiconductor photocatalysis has attracted a great deal of research attention due to its potential application to solve environmental problems [1, 2]. Among the various semiconductors employed, TiO_2 is a versatile material and good photocatalyst for the degradation of environmental contaminants due to its high photocatalytic avtivity, absence of toxicity, relatively low cost, and excellent chemical stability under various conditions [3, 4]. The excellent photocatalytic property of TiO_2 is due to its wide band gap and the long lifetime of photogenerated holes and electrons. With an appropriate light source, the TiO_2 photocatalyst generates electron/hole pairs to initiate a serious of chemical reactions that eventually mineralize the pollutants [5, 6]. As another photocatalyst, ZnO has unique electrical and optical properties that have many important applications, such as for transparent conducting films, waveguides, ultraviolet lasers, solar cells, photocatalysts, and varistors [7]. In particular, it has played an important role as a semiconductor for photocatalytic degradation of environmental pollutants, because its photodegradation mechanism has been shown to be similar to that of TiO_2 [8, 9]. The band gap energy of ZnO is similar to that TiO_2 (approximately 3.2 eV) [10].

Since a photocatalytic process is based on the generation of electron/hole pairs by means of band-gap radiation, the coupling of different semiconductor oxides seems useful to achieve a more efficient electron/hole pair separation under irradiation and a higher photocatalytic activity [11]. Thus, it is possible to enhance the activity of a TiO_2 photocatalyst by means of ZnO coupling. Moreover, the electronic exitation of TiO_2 nanoparticles needs a higher input energy when the particle size decreases because of the quantum size effect [12]. Therefore, it is highly desirable to synthesize TiO_2 nanoparticles with a high photocatalytic activity. TiO_2/ZnO nanocomposites have strong physical and chemical interactions with adsorbed species and have a variety of applications as gas sensing materials, thermoelectric materials, dye-sensitized solar cells, piezoelectric devices, and semiconductor photocatalyst [13-17].

The physical, chemical, and photochemical properties of the TiO_2/ZnO composites formed are dependent on the manufacturing method. To enhance the photodegradation efficienty of TiO_2 catalyst, coupled semiconductor photocatalysts TiO_2/ZnO have been prepared by several different processes, such as a solid-state reaction method [11, 14], thermal evaporation [12, 13], a hydrothermal reaction [18, 19], magnetron sputtering [19, 20], templating [22], electro spinning [23] and a sol-gel process [17, 24-27]. For a large variety of coupled nanocrystalline TiO_2/ZnO systems, the particles adhere to each other in so-called sandwich structures or present a core/shell geometry. There are some investigations on core/shell structured TiO_2/ZnO. Zhang *et al*. [12] suggested that anatase TiO_2/ZnO nanoparticles at a size of 6 nm were immobilized on single-crystalline tetrapod-like ZnO with dimensions up to 20-50 μm produced by a vapor hydrolysis method. The sol-gel process has notable advantages such as high purity, good uniformity of the microstructure, low temperature synthesis, easily controlled reaction condition, and hence has been widely adopted for preparing nanostructured TiO_2/ZnO composite.

However a few studies have been focused on the sol-gel system combined with polymerization complex method.

*Corresponding author:
Tel : +82-41-6601445
Fax: +82-41-6601445
E-mail: cslim@hanseo.ac.kr

In this study, ZnO nanoparticles were coated with TiO_2 nanolayers by a simple wet chemical route. Generally, in order to maintain high phtocatalytic properties, the inorganic particles should be small and highly distributed uniformly with a spherical particle morphology. In this study, nanocrystlline TiO_2 coated ZnO particles were synthesized by two-step chemical method. ZnO nanopartices were synthesized via polymerization complex method, and TiO_2 nanolayers were coated on the surface of ZnO nanoparticles by a sol-gel route. The nanocomposite TiO_2/ZnO prepared was characterized in detail by means of TG/DTA, XRD, SEM, EDS and TEM.

Experimentals

Nanocrystlline TiO_2 coated ZnO particles were synthesized by a two-step chemical method. ZnO nanopartices were prepared by a polymerzation complex method and TiO_2 nanopowders by a sol-gel method. For the ZnO nanopartices by the polymerzation complex method, zinc nitrate hexahydrate ($Zn(NO_3)_2{\cdot}6H_2O$, Junsei Chemical, Japan) was used as a metal cation source, citric acid (CA, $HOC(CO_2H)(CH_2CO_2H)_2$. Yakuri Oure Chemical, Japan) for a chelating agent and ethylene glycol (EG, $HOCH_2CH_2OH$, Tedia, USA) for a solvent. EG and CA with a molar ratio of 20 : 5 were heated in a microwave oven for 3 minutes in order to increase the solubility and mixed thoroughly until the mixture became a transparent solution without any observed precipitation. One mole of zinc nitrate hexahydrate was then added to this transparent solution and was mixed in the microwave oven until a transparent solution was once again obtained. The transparent reactants were stirred at 200 °C for 3 h inducing a polyester reaction. During this time the solution transformed gradually from a transparent liquid to a highly viscous black gel. The polymeric precursor was obtained by heating this polymerized complex in a drying oven at 250 °C for 24 h. ZnO nanoparticles were obtained after a calcination process at a temperature of 700 °C for 24 h.

For the TiO_2 nanopowders produced by a sol-gel method, titanium tetra-isopropoxide(TTIP) was used as a metal precursor, and isopropyl alcohol (IPA) as a solvent. Both were mixed in a molar ratio of 1 : 10 and stirred for 1 hour. Another solution was prepared from a mixture of H_2O and IPA with a molar ratio of 10 : 1. This solution was then titrated into the TTIP-IPA solution and stirred for 2 h until a uniform colloidal TiO_2 sol was produced. The TiO_2 sol obtained was analyzed in the neutral pH range by thermogravimetry/differential thermal analysis (TG/DTA, SDT-2960 TA instrument, U.S.A.).

For the production of TiO_2 coated ZnO nanopowders, the difference in surface charges is associated with variations in pH to produce a uniform coating of colloidal TiO_2 on the surface of ZnO particles. TiO_2 sol is chemically very unstable in the neutral pH range and therefore it easily agglomerates when it transforms into the gel state. However, this instability can be controlled by adding an acid. The TiO_2 sol was maintained at pH 3 by adding HCl. The ZnO nanoparticles were mixed with IPA and HCl. The TiO_2 sol yielded 5.5% of crystallized particles after volatilization of the organic species, H_2O and alcohol radicals during the heat treatment. Taking this percent yield into account, TiO_2 sol and IPA were mixed together in order to produce TiO_2 and ZnO particles with a weight ratio of 1 : 10. Mixing these components resulted in a colloidal suspension of ZnO and TiO_2.

The absorption process between the two heterogeneous particles was then initiated. After heat treatment in a drying oven at 250 °C for 24 h, TiO_2 coated ZnO nanoparticles were obtained by calcination at 500 °C for 3 h. The crystallization temperature, particle size and morphology were investigated using an X-ray diffractometer(XRD, Rigaku Denki, Japan, 40 kV, 30 mA, 5 $minute^{-1}$), scanning electron microscopy (SEM, JSM-5900LV, JEOL, Japan) and energy dispersive x-ray spectroscopy(SEM-EDS). Furthermore, transmission electron microscopy (TEM, 2000FX2, JEOL, Japan) and selected area electron diffraction(TEM-SAED) were employed to investigate the coating state and composite particle morphology.

Results and Discussion

Fig. 1 shows the difference in surface charges associated with variations in the pH. Heterogeneous particles, which are electrically charged with '+' and '−', bond interdependently by strong Coulomb attraction, and the degree of agglomeration is related to the neutralization of these charges. The variation in zeta potential of ZnO in Fig 1(a) and TiO_2 (b) with pH exhibited their isoelectric points (IEP) at 9.3 and 3.5, respectively. In order to obtain a maximum surface charge difference between the ZnO and TiO_2 particles, NH_4OH was added until a neutral pH was obtained (this was the average between the pH state of the two solutions). Fig. 2 shows the TG-DTA curves for the TiO_2 sol heated from room temperature to 900 °C in air. The weight loss begins above 300 °C and continues up to 450 °C, resulting from the evaporation and the combustion of organic species. This region corresponds to the DTA result of an

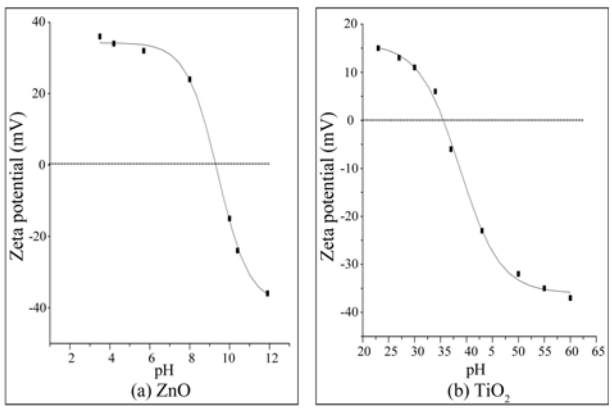

Fig. 1. The variation of the zeta potential with pH value showing the isoelectric points (IEP) at (a) pH 9.3 of ZnO and (b) pH 3.5 of TiO_2, respectively.

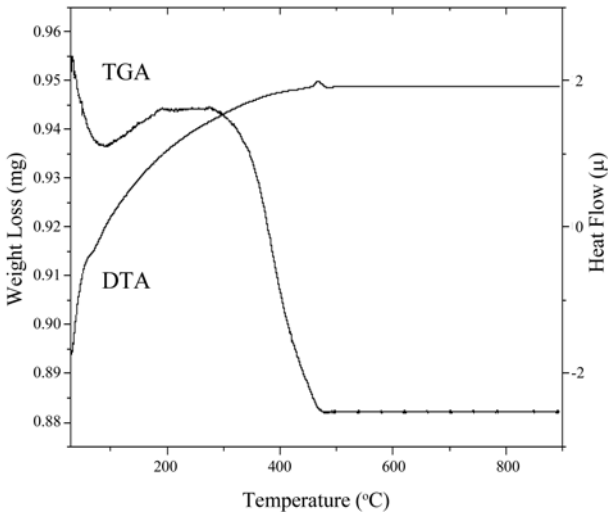

Fig. 2. TG-DTA curves for the TiO_2 sol heated from room temperature to 900 °C in air.

exothermic peak for the crystallization of TiO_2. It is assumed that the nuclei of TiO_2 produced near 450 °C and the growth of particles was propagated with increasing temperature.

Fig. 3 shows XRD result of the prepared ZnO particles heat-treated at 700 °C. The crystalline peaks marked by their Miller indices (100), (002), (101), (102), (110), (103), (200), (112), (201), (004) and (202) were identified as a pure hexagonal ZnO with a wurtzite structure (JCPDS no. 36-1451). Fig. 4 shows TEM images of (a) ZnO particles prepared by the polymerization complex method heat treated at 700 °C, and (b) TiO_2 particles by the sol-gel method heat-treated at 500 °C. The ZnO particles in Fig. 4(a) show a uniformly spherical shape with a size of 120-140 nm, while the TiO_2 particles in Fig. 4(b) show a homogeneous morphology with a size of 10-20 nm, approximately.

Fig. 5 shows XRD patterns of the TiO_2 coated ZnO nano particles prepared at 500 °C indicating the A (anatase TiO_2), R (Rutile TiO_2) and Z (ZnO). After TiO_2 coating, the XRD pattern had some significant changes and characteristic peaks for anatase and rutile TiO_2 crystalline were observed. The 2 theta peaks at about 31°(100), 34°(002) and 36°(101) represent the major peaks of ZnO and a major peak of the metastable anatase TiO_2 phase at 25°. On the other hand, the peaks of the stable rutile TiO_2 phase, which is more stable at higher temperatures, are weaker than the peaks from the antase phase.

Fig. 6 shows a SEM image of TiO_2 coated ZnO nano-

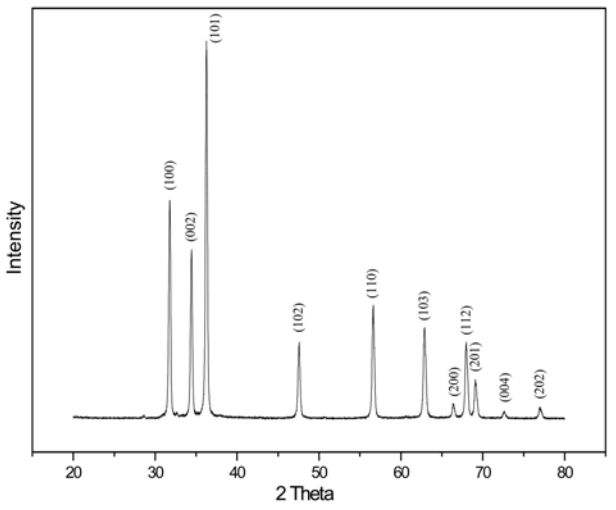

Fig. 3. XRD result of the prepared ZnO particles heat-treated at 700 °C.

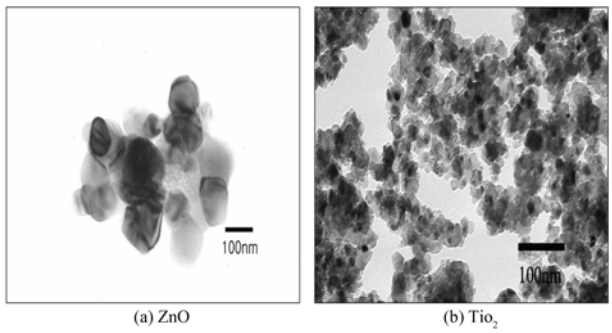

Fig. 4. TEM images of (a) ZnO particles prepared by the polymerization complex method heat treated at 700 °C, and (b) TiO_2 particles by the sol-gel method heat-treated at 500 °C.

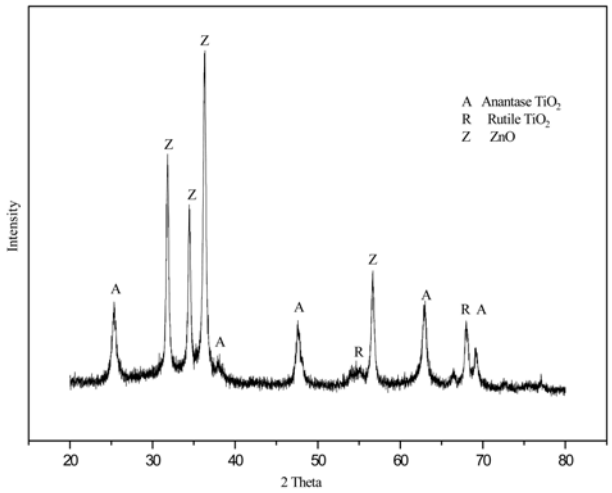

Fig. 5. XRD patterns of the TiO_2 coated ZnO nanoparticles prepared at 500 °C indicating peaks from the A (anatase TiO_2), R (Rutile TiO_2) and Z (ZnO).

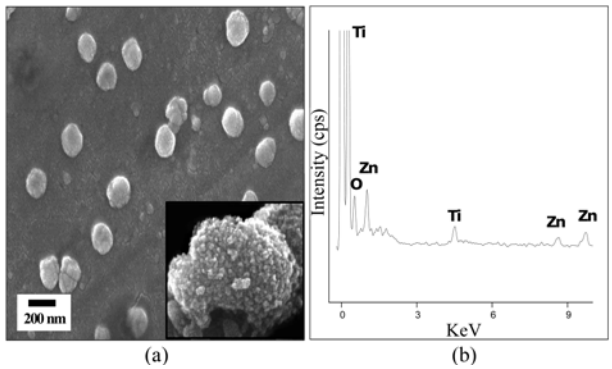

Fig. 6. SEM image of TiO_2 coated ZnO nanoparticles (a) and compositional data using EDS (b). The insert shows at high magnification the morphology of a TiO_2 coated ZnO nanoparticles.

particles (a) and compositional data using EDS (b). The insert in Fig. 6(a) shows at high magnification the morphology of a TiO_2 coated ZnO nanoparticle. The SEM image of the ZnO particles coated with TiO_2 nanoparticles in Fig. 6(a) shows a uniformly dispersed morphology with a size of 120-140 nm, without any agglomeration. It is emphasized, that the driving force controlling this coating process as described in Fig. 1, is electrical, as a consequence of Coulomb attraction resulting from induced charges on each component in the neutral pH region. The driving force for the heterogeneous bonding between the ZnO and TiO_2 particles was Coulombic attraction which is interdependant of the respective surface charge of each component. Also, as confirmed from the EDS results in Fig. 6(b), the particle is composed of TiO_2 and ZnO without any impurity.

Fig. 7 shows a TEM image and SAED patterns in the insert of a TiO_2 coated ZnO particle. The TEM image in Fig. 7 reveals that the resultant TiO_2 coated ZnO particle is discrete essentially with a mean diameter of about 120-140 nm. The thickness of the ZnO shell was 10 nm. It is observed that the darker ZnO core is surrounded by the lighter TiO_2 shell. Individual particles exhibit a TiO_2 nanolayer on the ZnO surface and the shell thickness is about 10-20 nm. The SAED pattern in the insert is identified with the phases of TiO_2 (Anatase), TiO_2 (Rutile) ZnO, ZnO/TiO_2. This is inaggreement with results of the XRD and EDS confirming this coexistence of crystalline TiO_2 and ZnO in each particle.

The coupling of TiO_2 coated ZnO nanoparticles like a layer-by-layer assembly is useful to achieve a more efficient electron/hole pair separation under irradiation and a higher photocatalytic activity [11]. It is possible to enhance the activity of a TiO_2 photocatalyst by means of ZnO coupling like the layer-by-layer assembly. The electronic exitation of TiO_2 nanoparticles needs a higher input energy when the particle size decreases because of the quantum size effect [12]. Therefore, it is highly desirable to synthesize TiO_2 nanoparticles with a high photocatalytic activity. The TiO_2/ZnO nanocomposites have strong physical and chemical interactions with adsorbed species and can support a variety of applications [13-17]. The coupled nanocrystalline TiO_2/ZnO particles adhere to each other in so-called sandwich structures or present a core/shell geometry. There are some investigations on core/shell structured TiO_2/ZnO. Zhang *et al*. [12] suggested that anatase TiO_2/ZnO nanoparticles at a size of 6 nm were immobilized on a single-crystalline tetrapod-like ZnO with dimensions up to 20-50 μm by a vapor hydrolysis method. The mechanism of this uniform deposition of TiO_2 nanoparticles on the surface of ZnO particles can be described as follows. Upon heating during the synthetic processing, the ethanol evaporates first since it has a low boiling point compared to water, and the vapor of water promoted the hydrolysis. The surface of ZnO acts as the nucleation sites during the initial stage of TiO_2 formation, and the as-formed TiO_2 nuclei subsequently act as the nucleation sites for further deposition of TiO_2 nanoparticles like the layer-by-layer assembling.

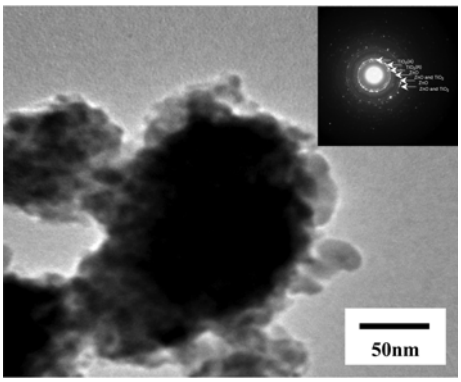

Fig. 7. TEM image and SAED pattern in the insert of a TiO_2 coated ZnO particle showing the darker ZnO core and the lighter TiO_2 shell surrounding it. The SAED pattern in the insert is identified with the phases of TiO_2 (Anatase), TiO_2 (Rutile), ZnO, ZnO/ TiO_2.

Conclusions

Nanocrystlline TiO_2 coated ZnO particles were successfully synthesized by a two-step chemical method, which were prepared by the polymerization synthesis of ZnO nanoparticles and followed by sol-gel coating of a TiO_2 nanolayer. The variation in zeta potential of ZnO and TiO_2 with pH exhibited their isoelectric points (IEP) at 9.3 and 3.5, respectively. ZnO nanoparticles are surrounded by the lighter crystalline TiO_2 layers. ZnO particles coated with TiO_2 nanoparticles show a uniformly dispersed morphology without any agglomeration. The average particle size of ZnO particles coated with TiO_2 particles was about 120-140 nm. The size of a ZnO nanoparticle was 100 nm and the thickness of the TiO_2 coating was below 10-20 nm. The driving force for the heterogeneous bonding between the ZnO and TiO_2 particles was Coulombic attraction which is interdependant on the respective surface charge of each component.

Acknowledgement

This research was supported by Basic Science Research Program through the National Research Foundation of Korea(NRF) funded by the Ministry of Education, Science and Technology (2010-0023911).

References

1. N.M. Dimitrijevic, Z.V. Saponjic, B.M. Rabatic and T. Rajh, J. Am. Chem. Soc. 127 (2005) 1344-1345.
2. B.M. Rabatic, N.M. Dimitrijevic and R.E. Cook, Adv. Mater. 18 (2006) 1033-1037.
3. S.J. Liao, D.G. Huang, D.H. Yu, Y.L. Su and G.Q. Yuan, J. Photochem. Photobiol. A 168 (2004) 7-13.
4. R. Comparelli, E. Fanizza, M.L. Curri, P.D. Corri, G. Mascolo and A. Agostiano, Appl. Cata. B 60 (2005) 1-11.
5. M. Muruganandham and M. Swaminathan, Energy Mater. Sol. Cells 81 (2004) 439-457.
6. L.Q. Jing, B.F. Xin, F.L. Yuan, B.Q. Wang, K.Y. Shi and

W.M. Cai, Appl. Catal. A 275 (2004) 49-54.
7. M.H. Cho and G.H. Lee, Thin Solid Films 516 (2008) 5877-5880.
8. C.Q. Ge, C.S. Xie, M.L. Hu, Y.H. Gui, Z.K. Bai and D.W. Zeng, Mat. Sci. Eng. B 141 (2007) 43-48.
9. Y. Zhou, W.B. Wu, G. Hu, H.T. Wu and S.G. Cui, Mat. Res. Bull. 43 (2008) 2113-2118.
10. C.C. Hsu and N.L. Wu, J. Photochem. Photobiol. A: Chem 172 (2005) 269-274.
11. K.H. Yoon, J. Cho and D.H. Kang, ibid. 34[9] (1999) 1451-1461.
12. Q. Zhang, W. Fan and L. Gao, Applied Catalysis B: Environmental 76 (2007) 168-173.
13. Y. Gui, S. Li, J. Xu and C. Li, Microeletronics Journal 39 (2008) 1120-1125.
14. K. Park and K.Y. Ko, J. Alloys and Compounds 430 (2007) 200-204.
15. S.K. Kansal, M. Singh and D. Sud, J. Hazarous Materials 153 (2008) 412-417.
16. E. Evgenidou, I. Konstantinou, K. Fytianos, I. Poulios and T. Albanis, Catalysis Today, 124 (2007)156-162.
17. D.L. Liao, C.A. Badour and B.Q. Liao, J. Photochem. Photobio. A: Chemistry 194 (2008) 11-19.
18. Y. Jiang, M. Wu, X. Wu, Y. Sun and H. Yin, Materials Letters, 63 (2009) 275-278.
19. C.W. Zou, X.D. Yan, J. Han, R.Q. Chen, J.M. Bian, E. Haemmerle and W. Gao, Che. Phy. Lett. 476 (2009) 84-88.
20. J.-L. Chung, J-C. Chen and C-J. Tseng, Applied Surface Science 255 (2008) 2494-2499.
21. J.-L. Chung, J.-C. Chen and C-J. Tseng, J. Physics and Chemistry 69 (2008) 535-539.
22. X. Li, K. Lv, K. Deng, J. Tang, R. Su, J. Sun and L. Chen, Mater. Sci. Eng. B 158 (2009) 40-47.
23. R. Liu, H. Ye, X. Xiong and H. Liu, Mat. Chem. Phys. in press (2010).
24. J. Tian, L. Chen, Y. Yin, X. Wang, J. Dai, Z. Zhu, X. Liu and P. Wu, Surf. Coat. Tech. 204 (2009) 205-214.
25. J. Tian, L. Chen, J. Dai, X. Wang, Y. Yin and P. Wu, Ceramics International 35 (2009) 2261-2270.
26. M.R. Vaezi, J. Materials Processing Technology 205 (2008) 332-337.
27. J. Qiu, Z. Jin, Z. Liu, X. Liu, G. Liu, W. Wu, X. Zhang and X. Gao, Thin Solid Films 515 (2007) 2897-2902.